ACS OMEGA

http://pubs.acs.org/journal/acsodf Article

Study on the Evolution of Fault Permeability and the Retention of Coal (Rock) Pillar under the Mining Conditions of Thick Coal Seam in the Footwall of Large Normal Fault

Huiyong Yin, Ruqian Tang, Daolei Xie,* Ning Lang, Shuo Li, Xiaorong Zhang, Yuxiao Cheng, Song Wang, and Anhao Li

Cite This: *ACS Omega* 2023, 8, 4187−4195 Read Online

ABSTRACT: As a typical geological structure, the fault often threatens the safe mining of coal mines. In order to investigate the permeability evolution of the significant normal fault under the mining disturbance of the thick coal seam of the fault footwall and to propose a scientific and reasonable coal (rock) pillar retention plan, this paper took the YinJiaWa Fault (YJW Fa), a large normal fault, in Fucun Coal Mine, Shandong Province, China, as a research object, conducted a coupled fluid and solid simulation study on permeability evolution of the fault using COMSOL Multiphysics, based on the revealed geological data and rock mechanical parameters, and combined the theoretical calculation results to determine the width of the waterproof coal (rock) pillar. The results show that the width of the waterproof coal (rock) pillar of YJW Fa is negatively correlated with the porosity, permeability, and flow velocity of each monitoring point. With the width of 60 m as the dividing point, as the width left less than 60 m and gradually reduced to 30 m, its water-blocking capacity is destroyed, increasing the seepage velocity in the water-flowing fractured zone, forming a water channel, causing water inrush accidents. The formula and numerical simulation results are used to determine the width of the waterproof coal (rock) pillar of the YJW Fa to be 74.44−84.08 m, to ensure the safe mining of the fault footwall. This paper provides a theoretical basis for further understanding of the fault permeability development rules and safety guidance for coal seam mining of the fault footwall.

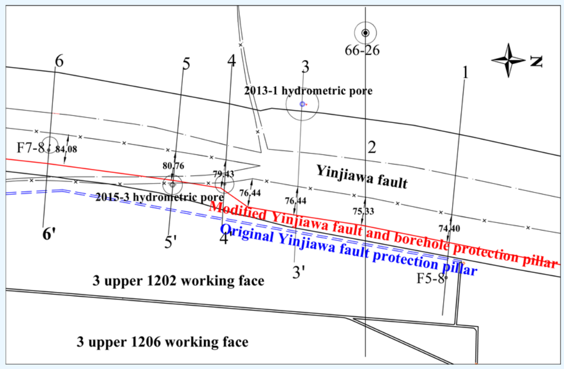

1. INTRODUCTION

Coal is the leading energy source in China and an important industrial raw material.[1,2] Many coal mines in China have complex geological conditions; the depth of mining has been increasing in recent years, and mine water disaster seriously restricts the safe and efficient production of coal mines,[3−5] among which fault water disaster occurs in high frequencies, is highly invisible, and causes particularly severe harm.[6−9] According to statistics, more than 80% of coal floor water inrush is caused by fracture structures such as faults.[10−16] As a typical geological structure during mine production, the fault, with crack development in the coal and rock near them and damage to the native rock structure and its integrity, is very likely to become water channels between the aquifer and the coal seam under mining disturbance conditions, posing the threat of water disaster to mine production and even causing water inrush accidents, leading to economic losses and casualties.[17] It can be seen that the fault water disaster is a severe threat to the safety of coal mine production, and it is necessary to conduct a series of studies on the fault permeability evolution and the retention of fault waterproof coal (rock) pillars.

Seepage in fractured rock is a typical two-way coupled fluid and solid process, where seepage can scour and carry away the tiny particles inside the fractured rock, causing the porosity and permeability of the fractured rock to increase continuously and the seepage velocity to increase. The increase in seepage velocity, in turn, accelerates the increase in porosity and permeability of the rock.[18] Chilingar et al.[19,20] summarized and optimized the equation for the relationship between permeability and porosity. Yao et al.[21,22] also simulated the formation process of seepage channels inside the collapse columns using COMSOL Multiphysics and summarized the time-varying rules of porosity, permeability, and flow velocity. Yang et al.[23,24] studied the seepage characteristics and evolution laws of broken rock mass. Hou et al.[25,26] studied

Received: November 15, 2022
Accepted: January 5, 2023
Published: January 18, 2023

https://doi.org/10.1021/acsomega.2c07325
ACS Omega 2023, 8, 4187−4195

the evolution law, variation characteristics, and internal relations of coal porosity and permeability. On the other hand, the study of fault activation mechanisms and waterproof coal (rock) pillar retention is the basis for ensuring safe production in mines near faults, conducted by many domestic and foreign scholars.[27] Islam et al.[28−30] carried out boundary element method analysis of fault activation law under the condition of roadway excavation disturbance and analyzed the activation rules of faults. Li et al.[31] explored the influence rules of the width of fault fracture zone on the critical value of coal pillars. Kun et al.[32−34] conducted a field and simulation research on the reasonable pillar width of extra thick coal seam. Yin et al.[35,36] summarized the current status of research on fault waterproof coal (rock) pillars and concluded that the research on fault coal pillars should be developed in the direction of multifield coupling, refinement, intelligence, and multimethod comprehensive research.

It can be seen from the above that scholars have mostly carried out research on the seepage characteristics of fractured rock using similar material tests and numerical simulations, but further research is needed on the influence of the width of the fault waterproof coal (rock) pillars on the porosity, permeability, and seepage field of the coal seam surrounding rock and the faulted rock. Therefore, this paper takes the YinJiaWa Fault (YJW Fa), a large normal fault, in Fucun Coal Mine, Shandong Province, China, as a research object. Based on the systematic collection of geological, hydrogeological, and mining data of the study area, a numerical model of the permeability of the mining coal seam surrounding rocks and the faulted rocks is established. The change in regularities of porosity, permeability, and flow velocity fields of the YJW Fa and coal seam surrounding rocks under different conditions of the width of the waterproof coal (rock) pillars of the fault are investigated. Also, the reasonable width of coal pillars under the combined influence of plastic collapse and deformation of coal seams under mining conditions still needs to be studied in depth, under the comprehensive consideration of the coal seam attitude and the influence arising from the spatial relationship of the tendency of the section and the coal seam. Therefore, this paper improves the formula for leaving the fault waterproof coal (rock) pillar in the "Water Control Rules for Coal Mines"[37] and selects a reasonable calculation result of the width of the coal (rock) pillar based on the safety, geological conditions, and the rules of influence of the width of the fault waterproof coal (rock) pillar on YJW Fa and coal seam surrounding rocks' internal porosity, permeability, and velocity field changes, which provide support for the practical design of the working face, the prevention and control of the fault water, and the protection of the coal mining.

2. PROJECT OVERVIEW

Fucun Coal Mine is located approximately 6 km northwest of Weishan County, Jining City, Shandong Province, China (Figure 1), and its geographical coordinates are the following: east longitude: 117°02′00″−117°04′19″; north latitude: 34°48′24″−34°53′34″.

The mine is mining the Shanxi Formation third upper and third lower coal seams, with a current production level of −480 m. The formation belongs to the North China stratigraphy. This paper takes the YJW Fa in the north of the east 12th working area of Fucun Coal Mine as the research object. The location of the research area is shown in the brown part of Figure 1. The east 12th working area is bound by the Fucun Reverse Fault to the south, the YJW Fa to the west, the Yaoqiao Fault to the north, and the branch fault of YJW Fa to the east, with a north−south tendency of 0−2.7 km long and an east−west tendency of 0−1.6 km wide, and the working area of about 2.39 km^2, mainly mining the third upper coal seam. The coal thickness in the northern area ranges from 2.08 to 3.0 m. The elevation of the third upper coal seam floor ranges from −296.34 to −412.1 m. The depth as a whole shows a trend of gradual increase from east to west and from north to south. As can be seen from Figure 2, the YJW Fa at the profile has a large fault throw of 276 m. YJW Fa is a normal fault, with the formations of upper wall relatively falling and the footwall relatively rising. On the section, the third upper coal seam of the footwall is all directly buttressed with the upper wall Jurassic conglomerate. The specific buttressed strata are as follows: the Jurassic aquifer in the upper wall of the fault is all buttressed with the footwall Jurassic conglomerate, sandstone of the lower stone box group, sandstone of the third coal roof, third upper coal seam, third lower coal seam, and so forth on the section. The water abundance of the Jurassic conglomerate aquifer is strong. According to the information of the Jurassic conglomerate hydrological exploration hole in the return tunnel of the east 12th working area, the borehole

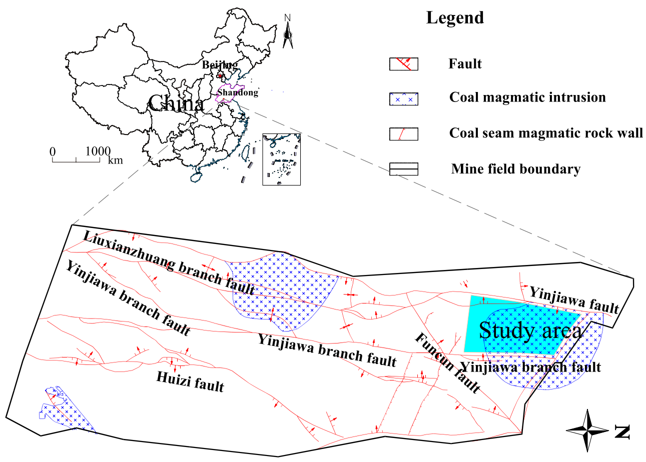

Figure 1. Location diagram of Fucun Coal Mine.

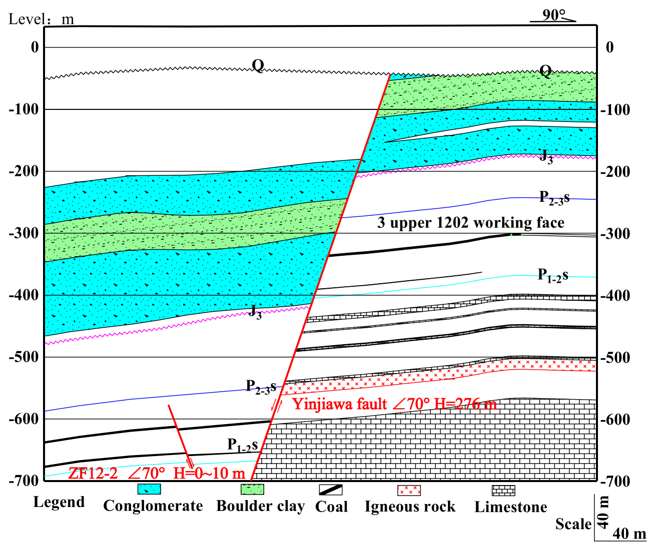

Figure 2. YJW Fa profile.

Table 1. Physical Mechanics and Seepage Parameters of Rock Strata

rock stratum	density (kg/m^3)	elastic modulus (GPa)	Poisson's ratio	porosity (%)	permeability (m^2)	viscosity of water (Pa·s)	unit weight of water (kN/m^3)
siltstone	2645	11.68	0.31	4.5	3.54×10^{-15}	0.001	9.8
fine sandstone	2730	10.05	0.32	6.2	5.41×10^{-14}		
conglomerate	2791	10.13	0.30	7.1	2.89×10^{-13}		
fault	2510	2.01	0.24	8.0	6.21×10^{-13}		
third upper coal seam	1564	2.35	0.30	4.3	2.83×10^{-15}		
fissure zone	2700	2.53	0.23	10.1	8.72×10^{-13}		

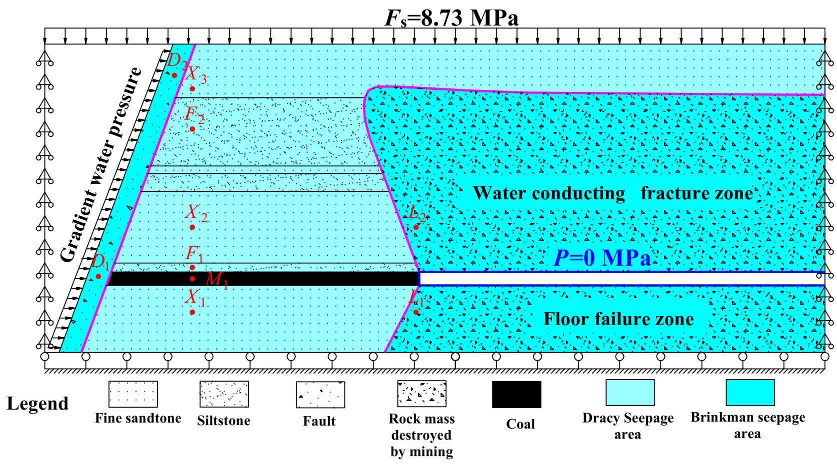

Figure 3. Numerical model of the surrounding rock and YJW Fa variable permeability in the coal seam near the fault mining.

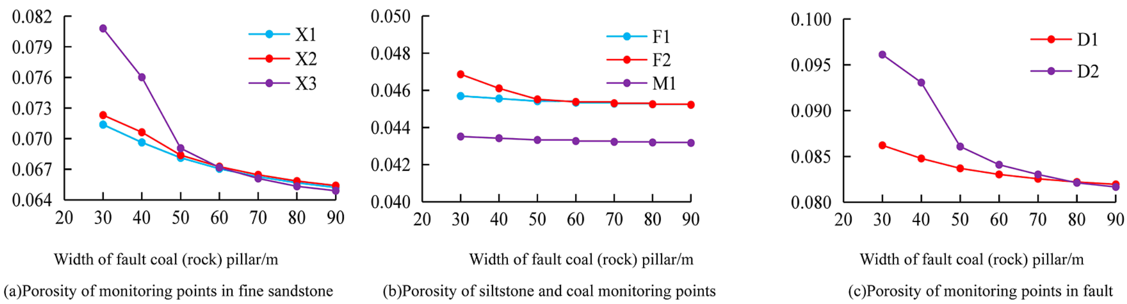

Figure 4. Relationship curve between the porosity of monitoring points and the setting width of coal (rock) pillar.

inflows are 49.5−98 m^3/h, which is very large. At present, the water level of the Jurassic conglomerate aquifer in the upper wall of the fault is −134.79 m, and the Jurassic water pressure in the third upper coal seam of the study area is 1.62−2.65 MPa. There is a possibility that the Jurassic conglomerate aquifer in the upper wall of the fault laterally recharges the sandstone aquifer in the third coal seam roof of the footwall, and the fault is very likely to become a water channel between the aquifer and the coal seam under mining disturbance conditions, which pose water disaster threat to mine production.

3. EVOLUTION LAW OF FAULT PERMEABILITY

3.1. Model Construction. Based on the data of the YJW Fa and two rock formations in the study area, the stratigraphic simplified model was constructed. The model length was 368 m, the height was 69 m, and the parameters of the geological force layer are shown in Table 1; the rock movement angle is 68°10′, as shown in Figure 3. Fixed constraints are applied at the bottom of the model, roller supports are applied on both sides of the boundary, and 8.73 MPa uniform load is applied at the upper boundary to simulate the self-gravity stress of the overlying stratum.

The regional seepage of YJW Fa, the water diversion fissure zone, and the bottom plate failure zone are controlled by the Brinkman equation, the groundwater seepage in the top bottom slate layer of the coal seam is controlled by the Darcy equation, and the seepage is controlled by gravity. A total of 10 monitoring points are set in the model to monitor the pressure, porosity, permeability, and flow rate changes of the coal seam roof, floor, and fault rock mass. The width of the coal (rock) pillar is continuously reduced during simulation and the evolution laws of porosity, permeability, and seepage field of coal seam roof, floor strata, and YJW Fa were explored at different widths of coal (rock) pillar of 90, 80, 70, 60, 50, 40, and 30 m.

3.2. Analysis of Numerical Simulation Results. The model calculation takes 150 days as the calculation time limit. It explores the changes in porosity, permeability, and velocity field of coal seam roof, floor, and fault under the conditions of different widths of waterproof coal (rock) pillar in 150 days.

https://doi.org/10.1021/acsomega.2c07325
ACS Omega 2023, 8, 4187−4195

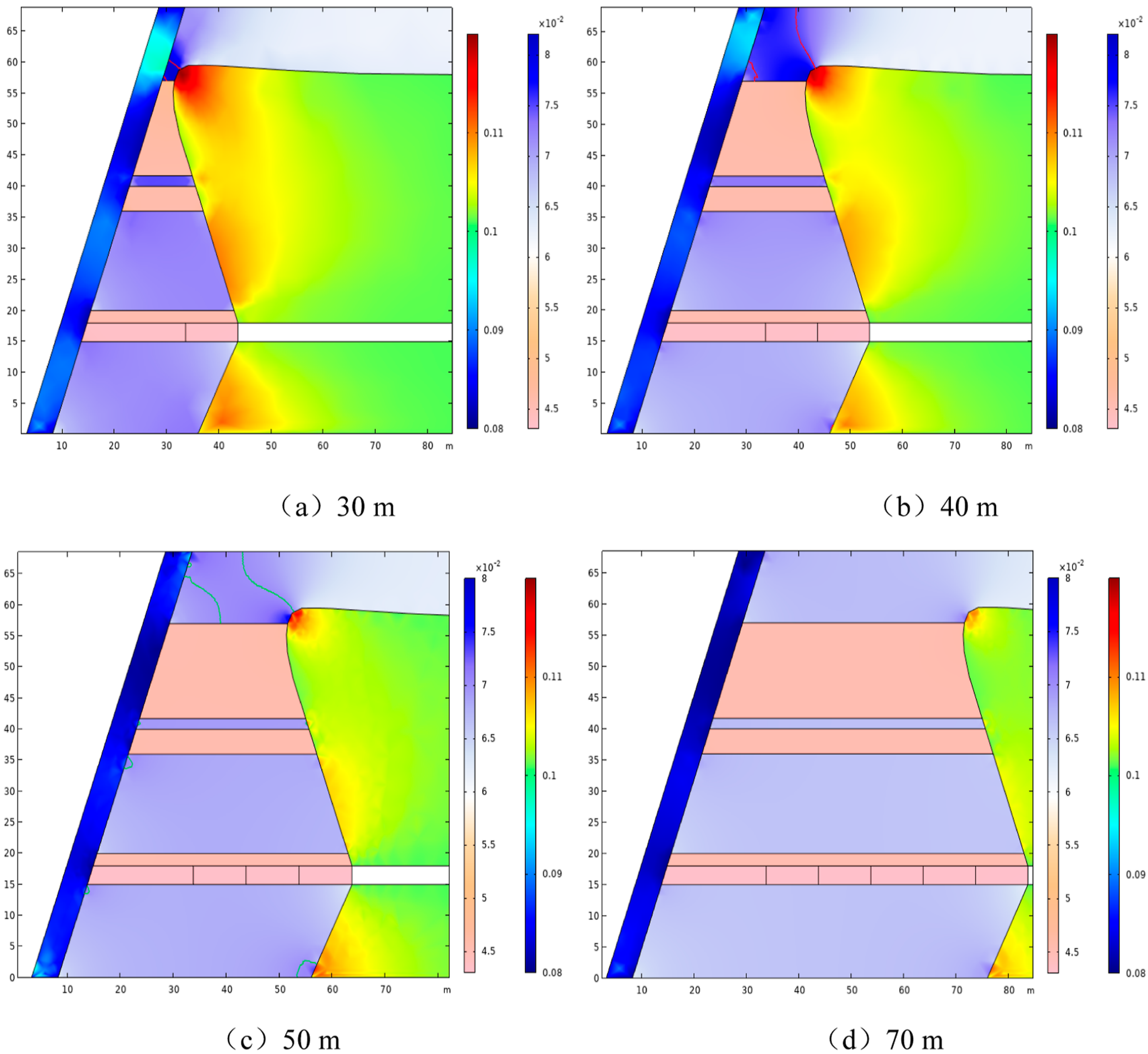

Figure 5. Porosity distribution at 50 m (left) and 70 m (right) width of coal (rock) pillar.

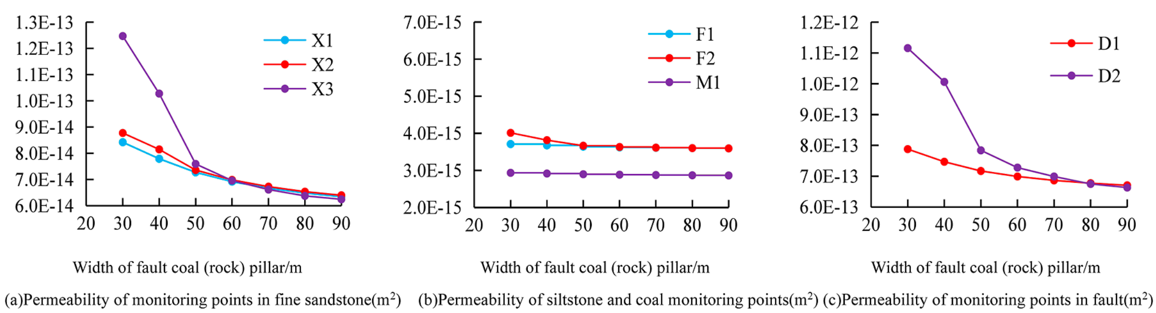

Figure 6. Relationship curve between the permeability of monitoring points and the setting width of fault coal (rock) pillar.

3.2.1. Evolution Law of Porosity under Different Widths of Coal (Rock) Pillar. From the relationship curve between the porosity of each monitoring point, the reserved width of the coal (rock) column (Figure 4), and the porosity distribution when the width of the coal (rock) column is 30, 40, 50, and 70 m (Figure 5), it can be seen that the porosity of the fault fractured rock mass in the layer connected with the fine sandstone changes significantly, which indicates that the water inrush channel is easier to occur in the fine sandstone than in the coal seam and siltstone. The reserved width of the coal

https://doi.org/10.1021/acsomega.2c07325
ACS Omega 2023, 8, 4187−4195

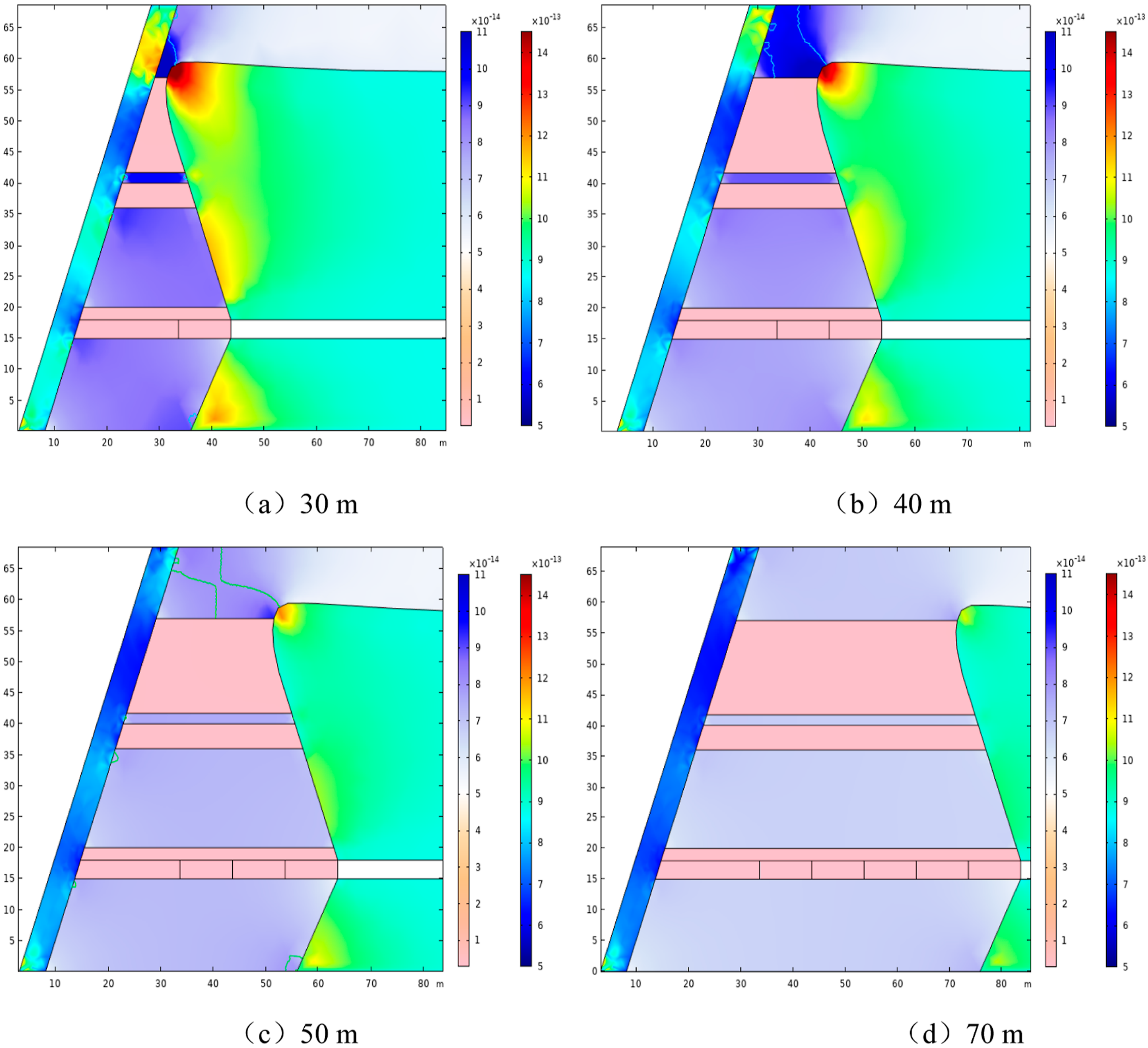

Figure 7. Permeability distribution at different widths of coal (rock) pillar: (left) (a) 30 m and (c) 50 m; (right) (b) 40 m and (d) 70 m.

(rock) pillar for water prevention and water isolation in YJW Fa has a negative correlation with the porosity of each monitoring point. The width of the coal (rock) pillar is 60 m as the dividing point. When the width is less than 60 m, the influence of the width of the coal (rock) pillar on the porosity is significantly enhanced. Moreover, under the influence of the water guide fracture zone, the fine sandstone at the top gradually forms a water guide channel through which Jurassic water can quickly enter the water guide fracture zone and then enter the working face, resulting in a water inrush accident. The threat of water damage to the production of the working face has further increased.

3.2.2. Evolution Law of Permeability under Different Widths of Coal (Rock) Pillar. The relationship curve between the porosity of each monitoring point and the width of the coal (rock) pillar is shown in Figure 6, and the distribution of porosity when the width of the coal (rock) pillar is 30, 40, 50, and 70 m is shown in Figure 7.

It can be seen from Figure 7 that the permeability evolution law and porosity are basically the same under the conditions of different widths of waterproof coal (rock) columns. The permeability of fault fractured rock mass at the seam butt joint with fine sandstone changes significantly, and the permeability of fine sandstone at the top and bottom of the coal seam changes more obviously than that of the coal seam and the siltstone; the reserved width of waterproof coal (rock) pillar in YJW Fa has a negative correlation with the permeability of each monitoring point. The evolution of the permeability with the width of the coal (rock) pillar can also be divided into two stages: slow growth and rapid growth. Taking the width of the coal (rock) pillar of 60 m as the dividing point, due to the influence of the water-conducting fracture zone, the permeability of the top fine sandstone increases significantly more than that of other formations, making it easier to generate water-conducting channels. As the width of the coal (rock) column decreases, the permeability of the top fine sandstone

https://doi.org/10.1021/acsomega.2c07325
ACS Omega 2023, 8, 4187−4195

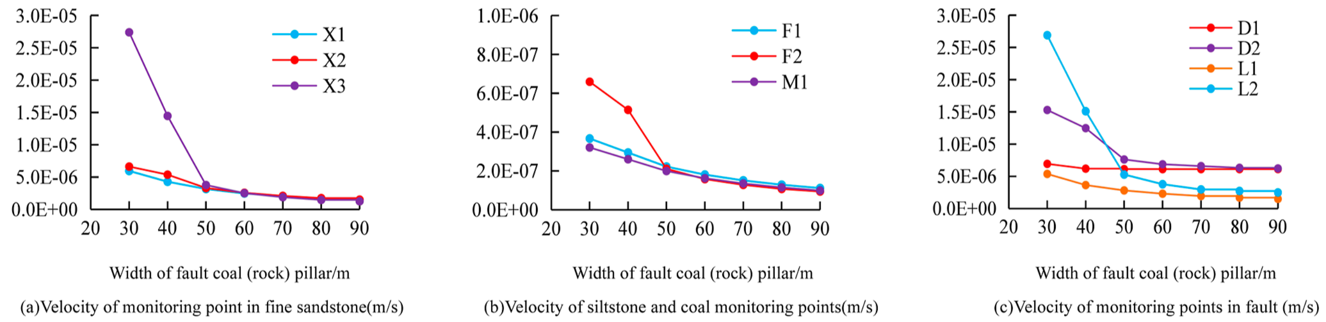

Figure 8. (a−c) Relationship curve between the flow velocity of monitoring points and the setting width of coal (rock) pillar.

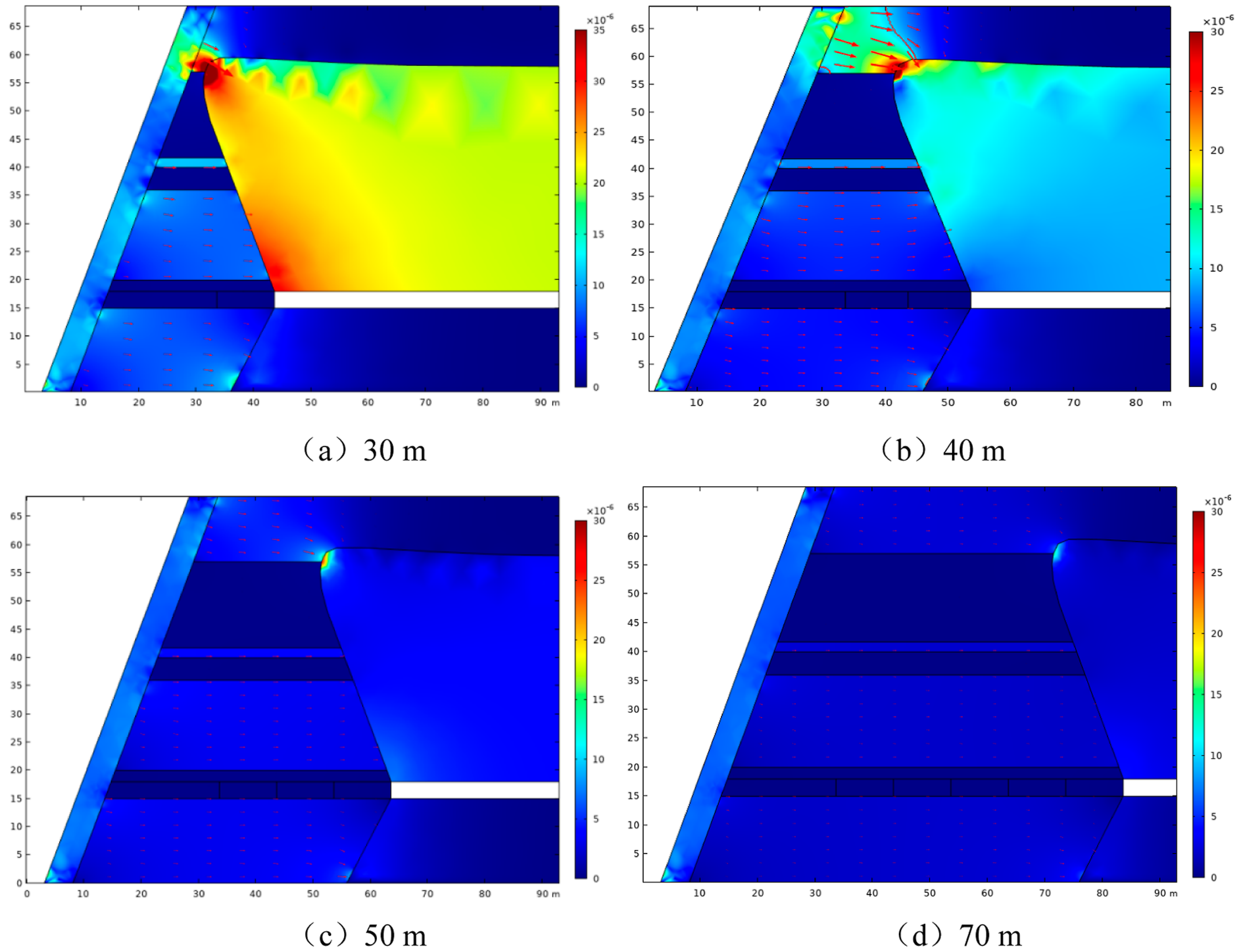

Figure 9. Flow velocity distribution at different widths of coal (rock) pillar: (left) (a) 30 m and (c) 50 m; (right) (b) 40 m and (d) 70 m.

gradually increases, and the water resistance of the coal (rock) column dramatically decreases.

3.2.3. Evolution Law of Flow Velocity Field under Different Widths of Coal (Rock) Pillar. According to the relationship curve between the flow velocity at each monitoring point, the reserved width of coal (rock) column (Figure 8), and the flow velocity distribution when the widths of the coal (rock) column are 30, 40, 50, and 70 m (Figure 9, the red arrow in the figure is the seepage direction), it can be found that the reserved width of waterproof coal (rock) column at YJW Fa has a negative correlation with the flow velocity at each monitoring point and in the absence of a seepage channel. The flow velocity of the water-conducting fracture zone (Brinkman seepage area) is higher than that of the coal seam roof and floor rock mass (Darcy seepage area); the internal seepage velocity and growth of fine sandstone are large, which is prone to roof water inrush. With the reserved width of waterproof coal (rock) pillar of YJW Fa being less than 60 m and gradually reduced to 30 m, its water blocking capacity is damaged, the porosity and permeability of the top fine sandstone are sharply increased, and the water permeability is greatly improved, resulting in an increase in

https://doi.org/10.1021/acsomega.2c07325
ACS Omega 2023, 8, 4187−4195

the seepage flow rate in the water guide fracture zone, forming a water guide channel, resulting in a water inrush accident.

According to the abovementioned change rules of porosity, permeability, and flow field, when the reserved width of waterproof coal (rock) pillar in YJW Fa is greater than or equal to 60 m, the width of coal (rock) pillar has little impact on the porosity, permeability, and flow field of coal seam roof, floor, and fault rock mass, and the water resistance capacity of coal (rock) pillar has not changed significantly; when the width of the coal (rock) pillar is less than 60 m, the influence of its width on the porosity, permeability, and flow velocity field of the coal seam roof, floor, and fault rock mass increases sharply. With the decrease of the width of the coal (rock) pillar, the porosity and permeability of the fine sandstone at the coal seam roof and floor increase rapidly, and the water permeability of the coal (rock) pillar increases rapidly, resulting in a rapid increase of the flow velocity. The increase of flow velocity further improves the scouring and migration of seepage on microparticles in the rock mass, which in turn increases the rate of porosity and permeability and is well reflected in the curve diagram of the relationship between porosity, permeability, and flow velocity at monitoring points and the reserved width of coal (rock) columns. Therefore, considering the influence of the width of coal (rock) pillar on the permeability, the reserved width of waterproof coal (rock) pillar in YJW Fa should be greater than or equal to 60 m.

4. SETTING OF WATER RESISTING COAL (ROCK) PILLAR IN FAULT

4.1. Reservation of Coal (Rock) Pillar for Water Prevention and Isolation of Fault When the Fault Contains Water or Conducts Water. According to the geological and hydrogeological conditions of the study area, the method of reservation of water-resisting coal (rock) pillar for water-bearing or water-conducting fault in Appendix 6-2 of the Detailed Rules for Water Prevention and Control in Coal Mines[37] is selected to calculate the water-resisting coal (rock) pillar for the footwall of YJW Fa in the study area, see Figure 10 for its schematic diagram and Formula 1:

$$L = 0.5Km\sqrt{\frac{3p}{K_p}} \geq 20\text{ m} \tag{1}$$

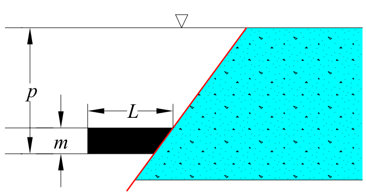

Figure 10. Water-bearing or water-conducting fault waterproof coal (rock) pillar retention.

where L is the reserved width of coal (rock) pillar, m; K is the safety factor, dimensionless, generally 2−5; m is the coal seam thickness or mining height, m; p is the actual head value, MPa; and K_p is the tensile strength of coal, MPa.

The values and sources of the calculation parameters are as follows: K, the safety factor, is taken as 5; M, the thickness or mining height of third upper coal seam in the study area is 2.08−3.0 m, and the value is 3.0 m; p, the actual water head of the Jurassic conglomerate aquifer at the floor elevation of third upper coal seam in the study area is 1.62−2.65 MPa (the water level of the Jurassic aquifer is −134.79 m, and the floor elevation of third upper coal seam in the study area is −296.34 to −399.9 m); and K_p, the tensile strength of coal is 0.51 MPa (according to the results of uniaxial tensile strength test of coal samples from third upper coal seam in Dongshi mining area of Fucun Coal Mine). According to calculation, the reserved width of waterproof coal (rock) pillar at each section is 25.09, 25.67, 26.25, 27.90, 28.60, and 30.29 m, respectively.

4.2. Improved Method for Setting Waterproof Coal (Rock) Pillar When the Coal Seam Contacts with a Strong Aquifer or Water Conducting Fault. The third upper coal seam in the study area is in contact with the Jurassic aquifer in the hanging wall of the YJW Fa. The top surface of the Jurassic conglomerate aquifer on the hanging wall of the fault is much higher than the maximum height of the water flowing fracture zone generated by the mining of the third upper coal seam in the study area. Moreover, the study area is located in the footwall of the fault, and the stratum and the fault are in the same direction. Therefore, the formula specified in the detailed rules for water prevention and control in coalmines is optimized in spatial geometry in this paper.

The schematic diagram of the waterproof coal (rock) column reserved in the contact between the improved coal seam and the strong aquifer or water-conducting fault is shown in Figure 11, and the improved calculation formula is shown in Formula 2:

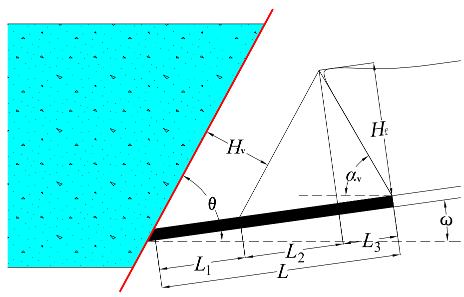

Figure 11. Fault waterproof coal (rock) column retaining when coal seam and fault are a synchronized combination.

$$\begin{aligned} L &= L_1 + L_2 + L_3 \\ &= H_s\ \csc(\theta - \omega) + H_f\ \cot(\theta - \omega) + H_f \\ &\quad \cot(\alpha_v + \omega) \end{aligned} \tag{2}$$

where L is the width of the waterproof coal (rock) column, m; H_f is the maximum height of the water-conducting fracture zone, m; θ is the fault dip angle (deg); ω is the apparent dip angle of coal seam on the vertical fault section (deg); α_v is the apparent movement angle of rock stratum on the vertical fault section (deg); and H_s is the width of the coal (rock) pillar for fault safety water prevention, (m). Among them, the width H_s of the coal (rock) pillar for fault safety and water prevention can be calculated by t Formula 3:

$$H_s = \frac{p}{T_s} + 10 \tag{3}$$

where p is the actual water head value, MPa and T_s is the critical water inrush coefficient, 0.1 MPa/m.

https://doi.org/10.1021/acsomega.2c07325
ACS Omega 2023, 8, 4187−4195

Through calculation, the slant lengths of waterproof coal (rock) columns in YJW Fa at each section are 74.89, 75.89, 76.90, 79.91, 81.25, and 84.59 m, respectively, and their horizontal projections (horizontal distance to the intersection of coal fault) are 74.44, 75.43, 76.44, 79.43, 80.76, and 84.08 m, respectively. When the improved coal seam contacts with the strong aquifer or the water-conducting fault, the retention of the waterproof coal (rock) pillar is more in line with the actual geological situation of the study area than before the improvement, and the calculated value is more conservative and safer.

Due to the influence of YJW Fa third upper coal seam in the footwall of the fault is in contact with the Jurassic aquifer in the hanging wall, the water in the Jurassic conglomerate aquifer has a certain impact on the mining of third upper coal seam in the study area. Combined with the research results of numerical simulation of the seepage change law of thick coal seam mining in the footwall of YJW Fa in Section 4, under the current geological conditions in the study area, the influence of water-conducting fracture zone on the evolution of coal (rock) column porosity, permeability, and flow velocity is more significant, and the possibility of roof water inrush in the working face is greater; when the width of waterproof coal (rock) pillar of YJW Fa is less than 60 m, with the decrease of the width of the coal (rock) pillar, the changes in porosity, permeability, and flow field in the coal seam roof, floor, and fault rock mass increase sharply, and the water resistance capacity of the waterproof coal (rock) pillar of the fault decreases greatly. When the width of the coal (rock) pillar is greater than or equal to 60 m, the width of the coal (rock) pillar has little impact on the porosity, permeability, and flow field of the coal seam roof and floor and the fault rock mass, and the water resistance ability of the fault waterproof coal (rock) pillar will not be damaged. Therefore, when the improved coal seam contacts with the strong aquifer or the water-conducting fault, the waterproof coal (rock) pillar retaining method is more in line with the geological and hydrogeological conditions of the study area than the other coal (rock) pillar retaining methods and is more safe and reasonable. It is comprehensively determined that the reserved width of waterproof coal (rock) column in YJW Fa is 74.44–84.08 m.

5. CONCLUSIONS

(1) COMSOL Multiphysics software is used to conduct numerical simulation research on the permeability evolution law of fault and coal seam top and bottom slate. The results show that the reserved width of waterproof coal (rock) pillar in YJW Fa has a negative correlation with the porosity, permeability, and flow velocity of each monitoring point. The width of the coal (rock) pillar is 60 m at the boundary point, and when the width is less than 60 m, the influence of the width of the coal (rock) pillar on it is obviously strengthened.

(2) The method of setting waterproof coal (rock) column when the coal seam contacts with the vital aquifer or water-conducting fault is improved, and the formula of setting waterproof coal (rock) column for fault considering the effect of water pressure is proposed. The width of setting waterproof coal (rock) column for YJW Fa is 74.44–84.08 m based on the formula and numerical simulation results to ensure the safe mining of the footwall of the fault. It provides safety guidance for the mining of other working faces affected by faults and is of great significance to the safety production of the mine.

■ AUTHOR INFORMATION

Corresponding Author

Daolei Xie – *College of Earth Science and Engineering and Shandong Provincial Key Laboratory of Depositional Mineralization & Sedimentary Mineral, Shandong University of Science and Technology, Qingdao 266590, China;* orcid.org/0000-0002-5363-095X; Email: skd994469@sdust.ede.cn

Authors

Huiyong Yin – *College of Earth Science and Engineering and Shandong Provincial Key Laboratory of Depositional Mineralization & Sedimentary Mineral, Shandong University of Science and Technology, Qingdao 266590, China;* orcid.org/0000-0002-2752-765X

Ruqian Tang – *College of Earth Science and Engineering and Shandong Provincial Key Laboratory of Depositional Mineralization & Sedimentary Mineral, Shandong University of Science and Technology, Qingdao 266590, China*

Ning Lang – *Shuifa Planning and Design Company Limited, Jinan 250100, China*

Shuo Li – *College of Earth Science and Engineering and Shandong Provincial Key Laboratory of Depositional Mineralization & Sedimentary Mineral, Shandong University of Science and Technology, Qingdao 266590, China*

Xiaorong Zhang – *College of Earth Science and Engineering and Shandong Provincial Key Laboratory of Depositional Mineralization & Sedimentary Mineral, Shandong University of Science and Technology, Qingdao 266590, China*

Yuxiao Cheng – *College of Earth Science and Engineering and Shandong Provincial Key Laboratory of Depositional Mineralization & Sedimentary Mineral, Shandong University of Science and Technology, Qingdao 266590, China*

Song Wang – *Zaozhuang Mining (Group) Fucun Coal Industry Company Limited, Zaozhuang 277519, China*

Anhao Li – *Shandong Lineng Luxi Mining Company Limited, Jining 272000, China*

Complete contact information is available at: https://pubs.acs.org/10.1021/acsomega.2c07325

Author Contributions

Resources, S.W. and A.L.; investigation, D.X.; writing—original draft, R.T. and H.Y.; supervision, Y.C.; funding acquisition, H.Y.; methodology, N.L.; format analysis, S.L. and X.Z. All authors have read and agreed to the published version of the manuscript.

Funding

This research was funded by The National Natural Science Foundation of Shandong Province, grant number [ZR2019MD013]. We thank Zaozhuang Mining (Group) Fucun Coal Industry Co., Ltd. for the data and information support and environmental geologists Dr. Wanfang Zhou, Dr. Fangying Dong, and Dr. Wenju Cheng for their useful discussions on the permeability of fault water.

Notes

The authors declare no competing financial interest.

https://doi.org/10.1021/acsomega.2c07325
ACS Omega 2023, 8, 4187–4195

■ REFERENCES

(1) Xie, H. P.; Wu, L. X.; Zheng, D. Z. Prediction on the energy consumption and coal demand of China in 2025. *J. China Coal Soc.* **2019**, *44*, 1949−1960.
(2) Cheng, W. J.; Dong, F. Y.; Tang, R. Q.; Yin, H. Y.; Shi, L. Q.; Zhai, Y. T.; Li, X. Improved Combination Weighted Prediction Model of Aquifer Water Abundance Based on a Cloud Model. *ACS Omega* **2022**, *7*, 35840−35850.
(3) Yin, H.; Wu, Q. Water Bursting Characteristic Analysis and Control Ways during Coal No.16 Winning in Binhu Coalmine, Tengzhou Mining Area. *Coal Geol. China* **2015**, *27*, 1674−1803.
(4) Shi, S. Q.; Wei, J. C.; Xie, D. L. Prediction analysis model for groundwater potential based on set pair analysis of a confined aquifer overlying a mining area. *Arabian J. Geosci.* **2019**, *12*, 115.
(5) Qiu, M.; Han, J.; Zhou, Y. Prediction Reliability of Water Inrush Through the Coal Mine Floor. *Mine Water Environ.* **2017**, *36*, 217−225.
(6) Yin, H. Y.; Sang, S. Z.; Xie, D. L. A numerical simulation technique to study fault activation characteristics during mining between fault bundles. *Environ. Earth Sci.* **2019**, *78*, 148.
(7) Zhou, Q. L.; Herrera, J.; Hidalgo, A. The Numerical Analysis of Fault-Induced Mine Water Inrush Using the Extended Finite Element Method and Fracture Mechanics. *Mine Water Environ.* **2018**, *37*, 185−195.
(8) Wu, Q.; Pang, W.; Dai, Y. C.; Yu, J. Vulnerability forecasting model based on coupling technique of GIS and ANN in floor groundwater bursting. *J. China Coal Soc.* **2006**, *3*, 314−319.
(9) Liu, W. T.; Han, M. K.; Meng, X. X.; Qin, Y. Y. Mine Water Inrush Risk Assessment Evaluation Based on the GIS and Combination Weight-Cloud Model: A Case Study. *ACS Omega* **2021**, *6*, 32671−32681.
(10) Tang, D. Q.; Wu, J. W.; Li, Y. C.; Hou, J. T. The features of fault zone rockmass engineering geologicalm echanics and its effect on leaving fault water proof pillar. *J. China Coal Soc.* **2006**, *31*, 455−460.
(11) Huang, H.-F.; Mao, X. B.; Yao, B. H.; Pu, H. Numerical simulation on fault water-inrush based on fluid-solid coupling theory. *J. Coal Sci. Eng.* **2012**, *18*, 291−296.
(12) Song, W.; Liang, Z. Z. Theoretical and numerical investigations on mining-induced fault activation and groundwater outburst of coal seam floor. *Bull. Eng. Geol. Environ.* **2021**, *80*, 5757−5768.
(13) Zhao, J. H.; Bo, B.; Juntao, J. T.; Ning, N. Mechanism of seepage-stress fault water inrush and grouting seal. *Arabian J. Geosci.* **2020**, *13*, 404.
(14) Li, L. P.; Li, S. C.; Shi, S. S.; Xu, Z. H. Water Inrush Mechanism Study of Fault Activation Induced by Coupling Effect of Stress-seepage-damage. *Chin. J. Rock Mech. Eng.* **2011**, *30*, 3295−3304.
(15) Liu, W. T.; Liu, S. L.; Liao, S. H. Study on Water Inrush Passage from Floor Affected by Fault. *Coal Eng.* **2015**, *47*, 85−88.
(16) Dong, F. Y.; Yin, H. Y.; Cheng, W. J.; Li, Y. J.; Qiu, M.; Zhang, C. W.; Tang, R. Q.; Xu, G. L.; Zhang, L. F. Study on water inrush pattern of Ordovician limestone in North China Coalfield based on hydrochemical characteristics and evolution processes: a case study in Binhu and Wangchao Coal Mine of Shandong Province, China. *J. Cleaner Prod.* **2022**, *380*, 134954.
(17) Shao, J.; Zhang, W. Q.; Wu, X. N.; Lei, Y.; Wu, X. T. Rock Damage Model Coupled Stress-Seepage and Its Application in Water Inrush from Faults in Coal Mines. *ACS Omega* **2022**, *7*, 13604−13614.
(18) Li, H.; Zhang, H. J.; Li, S. C. The seepage-flowing conversion mechanism of the fault lagging water inrush and its numerical simulation. *J. Min. Saf. Eng.* **2017**, *34*, 323−329.
(19) Chilingar, G. V. Relationship between porosity, permeability and grain size distribution of sands and sandsones. *Dev. Sedimentol.* **1964**, *1*, 71−75.
(20) Papamichos, E.; Vardoulakis, I. Sand erosion with a porosity diffusion law. *Comput. Geotech.* **2005**, *32*, 47−58.
(21) Yao, B. H. Research on variable mass fluid-solid coupling dynamic theory of broken rockmass and application. *J. China Univ. Min. Technol.* **2014**, *43*, 30−35.
(22) Zhang, K.; Wu, S. G. Study on the characteristics of variable mass seepage and water inrush mechanism of collapse column. *J. Min. Saf. Eng.* **2013**, *30*, 892−896.
(23) Yang, T. H.; Shi, W. H.; Li, S. C.; Yang, X.; Yang, B. State of the art and trends of water crush mechanism of nonlinear flow in fractured rock mass. *J. China Coal Soc.* **2016**, *41*, 1598−1609.
(24) Zhang, C.; Song, W. D.; Li, T.; Fu, J. X.; Li, Y. Study on stress seepage coupling model and numerical simulation of fractured rock mass. *J. Min. Saf. Eng.* **2021**, *38*, 1220−1230.
(25) Yin, X.*Study on Seepage Characteristics with Mass Loss of Broken Rock in Mountain Tunnel Containing Fault*; China University of Mining and Technology, 2018.
(26) Hou, H.; Qin, Q. H.; Liang, G. D.; Liang, G. D.; Tang, Y.; Zhang, H. J.; Li, Q. Q.; Liu, S. J. Study on the Applicability of Reservoir Fractal Characterization in Middle-High Rank Coals with NMR: Implications for Pore-Fracture Structure Evolution within the Coalification Process. *ACS Omega* **2021**, *6*, 32495−32507.
(27) Cai, W.; Dou, L. M.; Wang, G. F.; Hu, Y. W. Mechanism of fault reactivation and its induced coal burst caused by coal mining activities. *J. Min. Saf. Eng.* **2019**, *36*, 1193−1202.
(28) Islam, M. R.; Shinjo, R. Mining-induced fault reactivation associated with the main conveyor belt roadway and safety of the Barapukuria Coal Mine in Bangladesh: Constraints from BEM simulations. *Int. J. Coal Geol.* **2009**, *79*, 115−130.
(29) Ohnaka, M. Experimental studies of stick-slip and their application to the earthquake source mechanism. *J. Phys. Earth* **1973**, *21*, 285−303.
(30) Bailey, W. R.; Walsh, J. J.; Manzocchi, T. Fault populations strain distrution and basement fault reactivation in the East Pennines Coalfield UK. *J. Struct. Geol.* **2005**, *27*, 913−928.
(31) Li, P. F.; Liu, Q. M.; Chen, X. Y. Research on influence of width of fracture zone on fault activation and design of coal pillar. *J. Saf. Sci. Technol.* **2017**, *13*, 36−41.
(32) Kun, Z.; Ji, M.; Hongjin, G.; Wenrui, H. Study on reasonable width of coal pillar in thick coal seam section. *J. Mines, Met. Fuels* **2019**, *67*, 99−104.
(33) He, W.; He, F.; Zhao, Y. Field and simulation study of the rational coal pillar width in extra-thick coal seams. *Energy Sci. Eng.* **2019**, *8*, 627−646.
(34) Yang, K.; Gou, P. F. Research on Reasonable Width of Coal Pillars in High Strength Mining Roadway in Wantugou Mine. *Geotech. Geol. Eng.* **2021**, *39*, 2065−2073.
(35) Yin, H. Y.; Zhai, Y. T.; Zhao, C. Y.; Shi, Y. L.; Zhi, H. F. Research Status and Prospect of Fault Waterproof Coal (Rock) Column Design in China. *Saf. Coal Mines* **2020**, *51*, 187−191.
(36) Yin, H. Y.; Lang, N.; Zhou, X. L. Comprehensive Evaluation of Fault Hydraulic Conductivity Based on Fault Sealing and Numerical Simulation. *Saf. Coal Mines* **2022**, *53*, 200−207.
(37) National Coal Mine Safety Administration. *Detailed Rules for Prevention and Control of Water in Coal Mines*; China Coal Industry Publishing House, 2018.

https://doi.org/10.1021/acsomega.2c07325
ACS Omega 2023, 8, 4187−4195